Surface morphology and magnetic property of wrinkled FeGa thin films fabricated on elastic polydimethylsiloxane

Shuanglan Zhang,[1] Qingfeng Zhan,[1,a)] Ying Yu,[1,2] Luping Liu,[1] Huihui Li,[1] Huali Yang,[1] Yali Xie,[1] Baomin Wang,[1] Shuhong Xie,[2] and Run-Wei Li[1,a)]
[1]*Key Laboratory of Magnetic Materials and Devices and Zhejiang Province Key Laboratory of Magnetic Materials and Application Technology, Ningbo Institute of Materials Technology and Engineering, Chinese Academy of Sciences, Ningbo 315201, People's Republic of China*
[2]*Key Laboratory of Low Dimensional Materials and Application Technology of Ministry of Education, School of Materials Science and Engineering, Xiangtan University, Xiangtan, Hunan 411105, People's Republic of China*

(Received 29 January 2016; accepted 1 March 2016; published online 11 March 2016)

We investigated the surface morphology and the magnetic property of wrinkled $Fe_{81}Ga_{19}$ (FeGa) thin films fabricated in two different processes onto elastic polydimethylsiloxane (PDMS) substrates. The films obtained by directly depositing Ta and FeGa layers on a pre-strained PDMS substrate display a sinusoidally wrinkled surface and a weak magnetic anisotropy. The wavelength and amplitude of the sinusoidal morphology linearly increase with the metallic layer thickness, while the magnetic anisotropy decreases with increasing FeGa thickness. The other films grown by depositing FeGa layer on a wrinkled Ta/PDMS surface show a remarkable uniaxial magnetic anisotropy. The strength of magnetic anisotropy increases with increasing FeGa thickness. The magnetic anisotropy can be ascribed to the surface anisotropy, the magnetostrictive anisotropy, and the shape anisotropy caused, respectively, by the magnetic charges on wavy morphology, the residual mechanical stress, and the inhomogeneous thickness of FeGa films. © *2016 AIP Publishing LLC*. [http://dx.doi.org/10.1063/1.4943943]

Magnetic thin films exhibit distinct magnetic properties that are quantitatively and qualitatively different from those of their parent bulk materials. For magnetic films, the magnetic anisotropy determines their application area and the performance of devices using them. For example, the ferromagnetic resonance frequency for magnetic thin films applied in microwave devices depends on the magnetic anisotropy according to Kittel's equation.[1,2] In the application on magnetic sensors, the magnetic anisotropy of magnetic sensing layer has a remarkable influence on the magnetic field sensitivity.[3] Obviously, the control of magnetic anisotropy in magnetic thin films is critically important in the development of magnetic devices. Normally, there are several experimental methods to effectively manipulate the magnetic anisotropy in magnetic films, including oblique deposition,[4,5] field annealing treatment,[6] and interfacial exchange coupling.[7] Recently, a lot of works have modified the magnetic anisotropy by changing the surface morphology of magnetic thin films.[8–12] For instance, Chen *et al.* produced a rippled structure on the surface of Co films by means of ion beam etching and obtained a rather strong uniaxial magnetic anisotropy.[13] Ki *et al.* obtained a triangular wave-like morphology on m-plane Al_2O_3 substrate by a thermal annealing method, NiFe thin films deposited on this wavy surface display a significant magnetic anisotropy.[14]

In recent years, flexible magnetic thin films and devices have attracted numerous attentions because of their potential applications in wearable devices and stretchable electronics.[15–20] Due to the mismatch of Young's modulus between polymer substrate and metallic layer, metallic films grown on a pre-strained elastic substrate usually display a periodically wrinkled surface.[21–24] Briones *et al.* reported that self-assembled Co film deposited on a wrinkled elastomeric polydimethylsiloxane (PDMS) substrate exhibits a uniaxial magnetic anisotropy of 1.0×10^5 erg/cm^3.[25] So far, there is no systematical investigation on the influence of fabrication process on the surface morphology and the magnetic anisotropy of this kind of self-assembled wrinkled films. In this work, we selected $Fe_{81}Ga_{19}$ (FeGa) alloy, which exhibits the largest magnetostriction (~350 ppm for the typical bulk) among the various alloys not containing rare earth elements,[26–28] as the magnetic layer and studied the surface morphology and the magnetic anisotropy of wrinkled magnetic films deposited in different processes onto elastic PDMS membranes. FeGa films directly deposited on a pre-strained PDMS exhibit a topography with well-defined wrinkles and a weak uniaxial magnetic anisotropy. In contrast, the growth of FeGa layers on wrinkled Ta/PDMS surfaces leads to the irregularity of the periodical surface structure, but gives rise to a remarkable uniaxial magnetic anisotropy. The magnetic anisotropy of wrinkled FeGa/Ta/PDMS films can be interpreted by the surface anisotropy, the magnetostrictive anisotropy, and the shape anisotropy, respectively, due to the magnetic charges on the wrinkled surface, the residual mechanical stress, and the inhomogeneous thickness of FeGa films.

We fabricated patterned FeGa magnetic thin films on elastic PDMS membranes by using two different ways. For method A, as shown in Fig. 1(a), the PDMS substrates with a thickness of 360 μm were stretched 30% by using a homemade stretching apparatus. Subsequently, a 3 nm Ta layer and a FeGa layer with the thickness ranging from 10 nm to

a)Electronic addresses: zhanqf@nimte.ac.cn and runweili@nimte.ac.cn

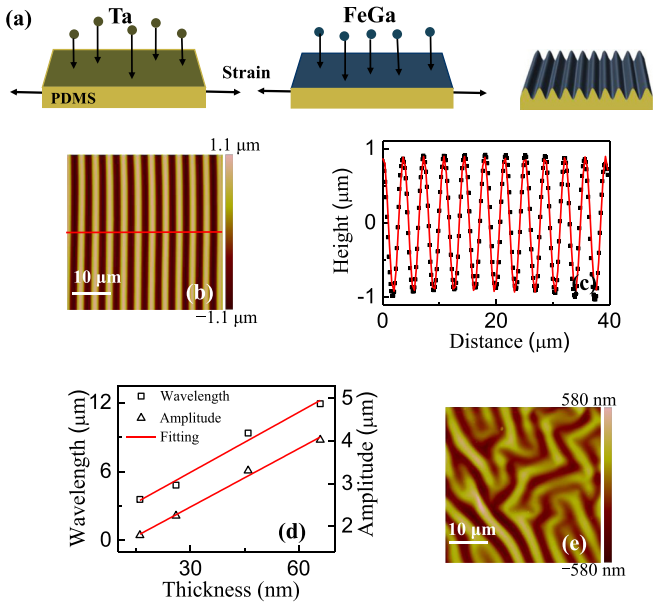

FIG. 1. (a) Schematic representation of method A used to fabricate wrinkled FeGa films. (b) 40 μm × 40 μm AFM image of 10 nm thick FeGa film with parallel wrinkles fabricated by using method A. (c) The cross-sectional view extracted along the red line shown in AFM image (black dot: measured results, red line: sinusoidal fitting). (d) The total thickness of FeGa and Ta layers dependence of the wavelength (open squares) and the amplitude (open uptriangles), the red lines are the linear fitting. (e) 40 μm × 40 μm AFM image for a 20 nm FeGa film grown on a freestanding PDMS without pre-strain.

60 nm were deposited on the pre-strained PDMS by using direct current magnetron sputtering. After the pre-strain was removed from the sample, an ordered wrinkled nanostructure appears on the surface. In method B, as shown in Fig. 2(a), a wrinkled morphology was first obtained by depositing a 3 nm Ta layer on 30% pre-strained PDMS. Then, FeGa films with various thicknesses were deposited on the relaxed Ta/PDMS patterned surface. Here, before depositing FeGa, a bottom layer of Ta was sputtered as a buffer layer to avoid FeGa atoms embedded into the soft substrates. Prior to be taken out of the sputtering chamber, a 3 nm Ta capping layer was deposited on FeGa films to avoid oxidation. During the deposition, we rotated the substrates to avoid directional sputtering. The base pressure of the sputtering chamber was smaller than 1×10^{-7} Torr. During the deposition of Ta and FeGa, the argon pressure was kept at 2.0×10^{-3} Torr. The thicknesses of Ta and FeGa films were controlled by the deposition time and were calibrated by X-ray reflectivity. The surface morphology was characterized by atomic force microscope (AFM, Veeco Dimension 3100 V). The hysteresis loops were measured by using a vibrating sample magnetometer (VSM, Lakeshore 7410) at various magnetic field orientations θ with respect to the wrinkles. The magnetic field was applied in the plane of film, and all the measurements were conducted at room temperature.

FeGa films obtained by using method A display a well-defined wrinkled morphology after releasing the 30% pre-strain, as typically shown in Fig. 1(c). The cross-sectional view of the wrinkled FeGa films can be well fitted to a sinusoidal curve, as revealed in Fig. 1(d). For the 10 nm thick FeGa film, the wavelength and the amplitude of the wrinkle pattern are characterized as 3.58 μm and 1.79 μm, respectively. With the thickness of FeGa layer increasing to 60 nm, the wavelength and the amplitude increase to 11.92 μm and 4.03 μm, respectively, as shown in Fig. 1(e). The formation of such a wrinkled surface is due to the mismatch of elastic modulus between the rigid metallic surface and the compliant elastomeric PDMS substrate. By means of minimizing the total strain energy consisting of the bending strain energy and the stretching strain energy in such a system, the wavelength λ and the amplitude h can be, respectively, described as[29–31]

$$\lambda \approx \frac{\pi t}{\sqrt{\varepsilon_c}},$$

$$h = t\left(\frac{\varepsilon_{PDMS}}{\varepsilon_C} - 1\right)^{1/2},$$

where $\varepsilon_c = 0.52\left[\frac{E_{PDMS}\left(1-\nu_M^2\right)}{E_M\left(1-\nu_{PDMS}^2\right)}\right]^{2/3}$ is a certain threshold strain for buckling and has to be exceeded for obtaining a wrinkle

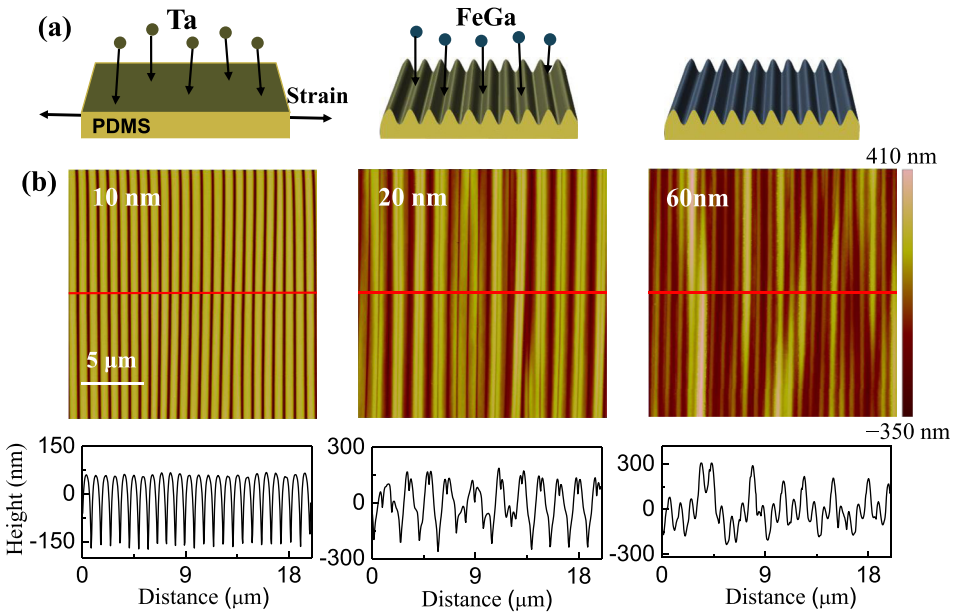

FIG. 2. (a) Schematic representation of method B used to fabricate wrinkled FeGa films. (b) 20 μm × 20 μm AFM images of FeGa films with 10 nm, 20 nm, and 60 nm in thickness fabricated by method B. The lateral profiles along the red line are shown below the AFM images.

pattern, t is the metallic layer thickness, ν_M and E_M are the Poisson ratio and the Young's modulus of metallic layers, ν_{PDMS} and E_{PDMS} denote the Poisson ratio and the Young's modulus of the PDMS, ε_{PDMS} is the pre-strain of PDMS substrates. It can be seen that the wavelength of wrinkles depends only on the thickness of metallic films and the film/substrate modulus ratio, but not on the pre-strain. The amplitude of wrinkles depends on both the film thickness and the pre-strain of PDMS. Since a pre-strain of 30% is used to grow all samples, the thickness dependent wavelength and amplitude of the wavelike topography can be linearly fitted, as shown in Fig. 1(d), where the film thickness includes both FeGa and Ta layers. The slopes of the fitting lines for the wavelength and the amplitude are about 174 and 40, respectively. Based on the previously reported elastic parameters for bulk alloys ($E_{FeGa} = 75$ GPa, $E_{Ta} = 100$ GPa, and $\nu_M = 0.30$) and PDMS membranes ($E_{PDMS} = 1$ MPa and $\nu_{PDMS} = 0.5$),[32–34] one can predict that the average theoretical slopes are 175 and 31 for the fitting of the wavelength and amplitude, respectively, which agree well with our experimental results in consideration of the difference of Young's modulus between metallic bulks and thin films.[35] It should be noted that when depositing FeGa on a freestanding PDMS without pre-strain, the film displays irregular wrinkles due to the random distribution of internal stress, as shown in Fig. 1(e). Such a FeGa film displays a magnetic isotropy.

For method B, a 3 nm Ta layer deposited on 30% pre-strained PDMS shows a wrinkled topography with a wavelength of 0.82 μm. After relaxing the pre-strain and depositing different thick FeGa films on the wrinkled Ta/PDMS patterns, the sinusoidal profile of the film surface gradually becomes irregular, but the wavelength determined by the 3 nm Ta buffer layer roughly remains unchanged, as shown in Fig. 2(b). For a 10 nm FeGa layer deposited on the wrinkled Ta/PDMS surface, the amplitude is 221 nm. With further increasing the nominal thickness of FeGa layer to 20 nm, two adjacent stripes bond together, the maximum amplitude increases to 437 nm. When the nominal thickness of FeGa layer increases to 60 nm, more stripes entangle together and the maximum amplitude reaches 532 nm. Obviously, the change of FeGa morphology is due to the deposition on the wrinkled Ta/PDMS surface, which makes the atomic flux display different incidence angles. Consequently, the FeGa thickness becomes locally inhomogeneous, which produces a residual stress and breaks the periodically wrinkled morphology. By increasing the nominal thickness, the FeGa film becomes even inhomogeneous. The residual stress is further enhanced and the stripes entangle together, which makes more complex structures.

The magnetic properties of the wrinkled FeGa films were measured at different magnetic field orientations, θ, with an increment of 10°. Figures 3(a) and 3(b) show the hysteresis loops for different thick FeGa films deposited on the 30% pre-strained PDMS membranes by using method A. For the measurement with magnetic field applied parallel to the wrinkles, i.e., $\theta = 0°$, with increasing FeGa thickness from 20 nm to 60 nm, the loop squareness M_r/M_s slightly decreases from 0.92 to 0.91, and the coercive field H_c changes from 41 Oe to 87 Oe. When the magnetic field is applied perpendicular to the wrinkles, i.e., $\theta = 90°$, the value of M_r/M_s correspondingly increases from 0.83 to 0.87 and H_c

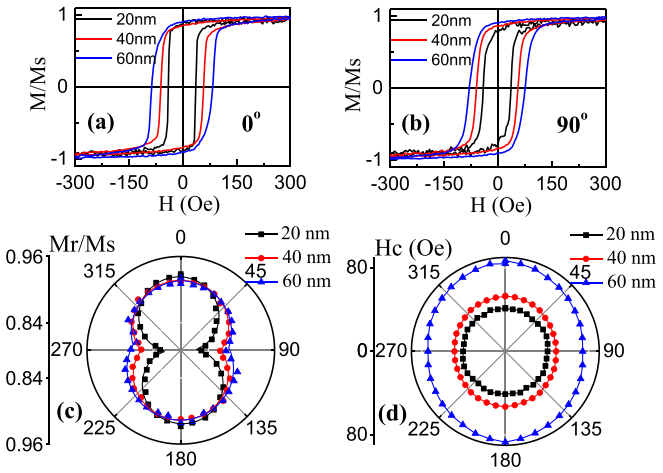

FIG. 3. Hysteresis loops for FeGa films with different thicknesses obtained by method A when the magnetic field is applied (a) parallel and (b) perpendicular to wrinkles. (c) Loop squareness M_r/M_s and (d) coercive field H_c as a function of the magnetic field orientation with respect to the wrinkles.

increases from 39 Oe to 74 Oe. Figures 3(c) and 3(d) summarize the angular dependence of M_r/M_s and H_c for FeGa films with different thicknesses, respectively. They both exhibit a uniaxial symmetry about the directions parallel or perpendicular to the wrinkles. The M_r/M_s ratio shows the maximum and minimum values at $\theta = 0°$ and $\theta = 90°$, respectively, indicating a uniaxial magnetic anisotropy with easy axis parallel to wrinkles and hard axis perpendicular to wrinkles. Figures 4(a) and 4(b) show the hysteresis loops for FeGa films deposited on the wrinkled Ta/PDMS surface by using method B. For $\theta = 0°$, by increasing the FeGa film thickness from 20 nm to 60 nm, the M_r/M_s ratio increases from 0.89 to 0.93 and the coercive field H_c changes from 75 Oe to 96 Oe. For $\theta = 90°$, the M_r/M_s ratio correspondingly decreases from 0.60 to 0.22 and H_c decreases from 47 Oe to 36 Oe. The angular dependence of M_r/M_s and H_c, as respectively shown in Figs. 4(c) and 4(d), exhibits a uniaxial symmetry, indicating a uniaxial magnetic anisotropy along the wrinkles. The uniaxial anisotropy K_u of FeGa films can be estimated from the difference of the area enclosed between the hysteresis loops

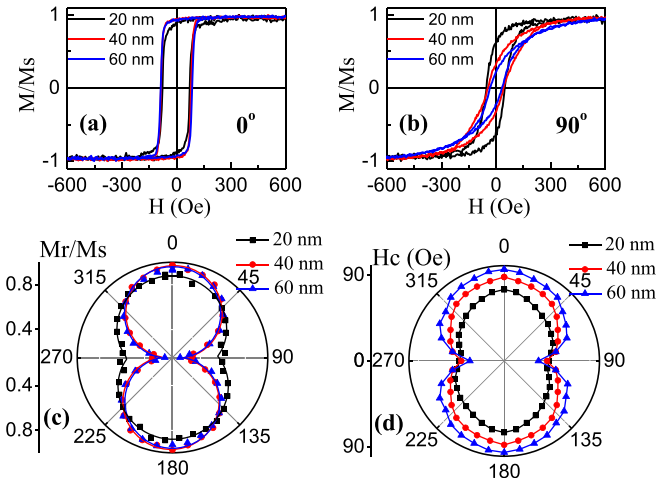

FIG. 4. Hysteresis loops of FeGa films with different thicknesses obtained by method B when the magnetic field is applied (a) parallel and (b) perpendicular to wrinkles. (c) Loop squareness M_r/M_s and (d) coercive field H_c as a function of the magnetic field orientation with respect to the wrinkles.

measured along the easy and hard axes.[25,36] The calculation indicates that FeGa films fabricated by method A show a very weak K_u, the strength decreases from 7.70×10^3 erg/cm^3 to 3.08×10^3 erg/cm^3 when the FeGa thickness increases from 20 nm to 60 nm. In contrast, FeGa films fabricated by method B display a rather strong K_u which increases from 4.40×10^4 erg/cm^3 to 1.28×10^5 erg/cm^3 with FeGa thickness increasing from 20 nm to 60 nm, as shown in Fig. 5(a).

The difference of magnetic anisotropy of the wrinkled magnetic films is due to the different magnetic anisotropy mechanisms caused by the different deposition processes. For method A, FeGa films were deposited on a pre-strained and flat PDMS substrate, so the film thickness is homogeneous. After relaxing the pre-strain, the wrinkles appear on the film surface. When a saturation magnetic field applied perpendicular to the wrinkles aligns the FeGa magnetization parallel to the film plane, magnetic charges are created on the film surface, as schematically shown in Fig. 5(b). The dipolar interaction between the magnetic charges acts as a coupling field favoring parallel alignment of magnetization.[13,15] As a result, a surface anisotropy with easy axis along the wrinkles is induced. Chen *et al*. developed a theoretical model to estimate the surface anisotropy for a wavy morphology with the amplitude smaller than the film thickness.[13] However, this model cannot precisely predict the surface anisotropy for our FeGa films with the amplitude by far larger than the FeGa thickness. Since the wavelength for the wrinkled FeGa films obtained by method A is several μm; in this length scale, the dipolar interaction between magnetic charges becomes very weak,[37] which would produce a weak surface anisotropy. In addition, the $1/t_{FeGa}$ behavior of K_u for FeGa films by method A confirms that the main contribution comes from the surface anisotropy (see Fig. 5(a)), the effect of residual stress on K_u can be neglected. For method B, the sinusoidally wrinkled morphology of Ta/PDMS makes the deposition of FeGa layer on this kind of surface displaying different incidence angles of atomic flux.[38] As a result, the FeGa thickness becomes no longer homogeneous, thus a residual stress is produced, resulting in the irregularity of the periodically wrinkled morphology. Therefore, for method B, the magnetic anisotropy is mostly contributed by both the residual stress-induced anisotropy via the magnetostrictive behaviors of FeGa and the shape anisotropy due to the inhomogeneous thickness of FeGa layer. The increase of K_u with FeGa thickness indicates the insignificant contribution of surface anisotropy by the wrinkled morphology.

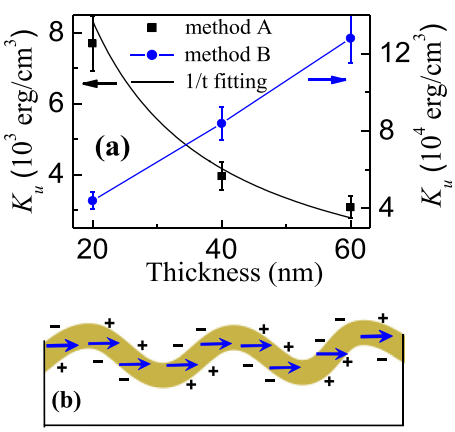

FIG. 5. (a) Black squares for method A and the blue dots for method B show the FeGa thickness dependence of the strength of uniaxial magnetic anisotropy K_u. The black line indicates the $1/t_{\mathrm{FeGa}}$ fitting for K_u obtained by method A. The blue line is a guide for the eye. (b) Surface magnetic charges are created due to the wrinkled film surface when the magnetization orientation in FeGa thin film is aligned perpendicular to the wrinkles.

In summary, we investigated the surface morphology and the magnetic property of wrinkled FeGa films produced on elastic PDMS by different fabrication processes. The films obtained by directly depositing Ta and FeGa layers on a pre-strained PDMS substrate display a sinusoidally wrinkled surface and a very weak magnetic anisotropy caused by the surface anisotropy due to the magnetic charges distributed on the wavy morphology. In contrast, the films by depositing FeGa on a wrinkled Ta/PDMS surface show a remarkable uniaxial magnetic anisotropy, which is mostly contributed by both the residual stress-induced anisotropy via the magnetostrictive behaviors of FeGa and the shape anisotropy due to the inhomogeneous thickness of FeGa layer.

The authors acknowledge the financial support from the National Natural Science Foundation of China (Nos. 11374312, 51401230, and 51522105) and Ningbo Science and Technology Innovation Team (2015B11001).

[1]C. Kittel, Phys. Rev. **71**, 270 (1947).
[2]N. N. Phuoc, P. Chapon, O. Acher, and C. K. Ong, J. Appl. Phys. **114**, 153903 (2013).
[3]E. Quandt and A. Ludwig, J. Appl. Phys. **85**, 6232 (1999).
[4]A. Lisfi, J. C. Lodder, H. Wormeester, and B. Poelsema, Phys. Rev. B **66**, 174420 (2002).
[5]X. Fan, D. Xue, M. Lin, Z. Zhang, D. Guo, C. Jiang, and J. Wei, Appl. Phys. Lett. **92**, 222505 (2008).
[6]J. H. Yoo, J. B. Restorff, M. Wun-Fogle, and A. B. Flatau, J. Appl. Phys. **103**, 07B325 (2008).
[7]B. K. Kuanr, R. E. Camley, and Z. Celinski, J. Appl. Phys. **93**, 7723 (2003).
[8]L. Thevenard, H. T. Zeng, D. Petit, and R. P. Cowburn, J. Appl. Phys. **106**, 063902 (2009).
[9]B. Ziberi, F. Frost, T. Höche, and B. Rauschenbach, Phys. Rev. B **72**, 235310 (2005).
[10]C. A. F. Vaz, S. J. Steinmuller, and J. A. C. Bland, Phys. Rev. B **75**, 132402 (2007).
[11]M. O. Liedke, M. Körner, K. Lenz, M. Fritzsche, M. Ranjan, A. Keller, and J. Lindner, Phys. Rev. B **87**, 024424 (2013).
[12]H. L. Liu, T. Škereň, A. Volodin, K. Temst, A. Vantomme, and C. Van Haesendonck, Phys. Rev. B **91**, 104403 (2015).
[13]K. Chen, R. Frömter, S. Rössler, N. Mikuszeit, and H. P. Oepen, Phys. Rev. B **86**, 064432 (2012).
[14]S. Ki and J. Dho, Appl. Phys. Lett. **106**, 212404 (2015).
[15]S. C. B. Mannsfeld, B. C. K. Tee, R. M. Stoltenberg, C. V. H-H. Chen, S. Barman, B. V. O. Muir, A. N. Sokolov, C. Reese, and Z. Bao, Nat. Mater. **9**, 859 (2010).
[16]C. Gao and B. Bhushan, Wear **190**, 60–75 (1995).
[17]J. Liang, Y. Xu, D. Sui, L. Zhang, Y. Huang, Y. Ma, F. Li, and Y. Chen, J. Phys. Chem. C **114**, 17465 (2010).
[18]Z. W. Liu, Y. Liu, L. Yan, C. Y. Tan, and C. K. Ong, J. Appl. Phys. **99**, 043903 (2006).
[19]M. Melzer, D. Karnaushenko, G. Lin, S. Baunack, D. Makarov, and O. G. Schmidt, Adv. Mater. **27**, 1333 (2015).
[20]M. Donolato, C. Tollan, J. M. Porro, A. Berger, and P. Vavassori, Adv. Mater. **25**, 623 (2013).
[21]Y. Wang, R. Yang, Z. Shi, L. Zhang, D. Shi, E. Wang, and G. Zhang, ACS Nano. **5**, 3645 (2011).
[22]C. Yu and H. Jiang, Thin Solid Films **519**, 818 (2010).
[23]J. W. Hutchinson, Philos. Trans. R. Soc. **371**, 20120422 (2013).
[24]K. Efimenko, M. Rackaitis, E. Manias, A. Vaziri, L. Mahadevan, and J. Genzer, Nat. Mater. **4**, 293 (2005).

[25]J. Briones, P. Toro, A. Encinas, L. Caballero, J. C. Denardin, F. Melo, E. Cerda, S. Robert, and F. Montaigne, Appl. Phys. Lett. **103**, 072404 (2013).
[26]T. Brintlinger, S. H. Lim, K. H. Baloch, P. Alexander, Y. Qi, J. Barry, J. Melngailis, L. Salamanca-Riba, I. Takeuchi, and J. Cumings, Nano Lett. **10**, 1219 (2010).
[27]M. Barturen, B. Rache Salles, P. Schio, J. Milano, A. Butera, S. Bustingorry, C. Ramos, A. J. A. de Oliveira, M. Eddrief, E. Lacaze, F. Gendron, V. H. Etgens, and M. Marangolo, Appl. Phys. Lett. **101**, 092404 (2012).
[28]X. S. Zhang, Q. F. Zhan, G. H. Dai, Y. W. Liu, Z. H. Zuo, H. L. Yang, B. Chen, and R. W. Li, J. Appl. Phys. **113**, 17A901 (2013).
[29]D. Y. Khang, H. J. Jiang, Y. Huang, and J. A. Rogers, Science **311**, 208 (2006).
[30]X. Chen and J. W. Hutchinson, J. Appl. Mech. **71**, 597 (2004).
[31]Z. Y. Huang, W. Hong, and Z. Suo, J. Mech. Phys. Solids **53**, 2101 (2005).
[32]F. M. Wun, J. B. Restorff, and A. E. Clark, IEEE Trans. Magn. **42**, 3120 (2006).
[33]Y. L. Zhou, M. Niinomi, and T. Akahori, Mater. Sci. Eng. **371**, 283 (2004).
[34]M. K. Chaudhury, J. A. Finlay, J. Y. Chung, M. E. Callow, and J. A. Callow, Biofouling **21**, 41 (2005).
[35]D. Son, J. Jeong, and D. Kwon, Thin Solid Films **437**, 182 (2003).
[36]M. T. Johnson, P. J. H. Bloemen, F. J. A. den Broeder, and J. J. de Vries, Rep. Prog. Phys. **59**, 1409 (1996).
[37]Q. F. Zhan, J. H. Gao, Y. Q. Liang, N. L. Di, and Z. H. Cheng, Phys. Rev. B **72**, 024428 (2005).
[38]Q. F. Zhan, C. Van Haesendonck, S. Vandezande, and K. Temst, Appl. Phys. Lett. **94**, 042504 (2009).